Hydrol. Earth Syst. Sci. Discuss., 7, 493–528, 2010
www.hydrol-earth-syst-sci-discuss.net/7/493/2010/

Hydrology and Earth System Sciences Discussions

This discussion paper is/has been under review for the journal Hydrology and Earth System Sciences (HESS). Please refer to the corresponding final paper in HESS if available.

Responses of snowmelt runoff to climatic change in an inland river basin, Northwestern China, over the past 50a

J. Wang, H.-Y. Li, and X.-H. Hao

Cold and Arid Regions Environmental and Engineering Research Institute, Chinese Academy of Sciences, Lanzhou 730000, China

Received: 18 December 2009 – Accepted: 5 January 2010 – Published: 21 January 2010

Correspondence to: J. Wang (wjian@lzb.ac.cn)

Published by Copernicus Publications on behalf of the European Geosciences Union.

Abstract

The spatial and temporal variations of snowcover distribution, and snowmelt runoffs are considered as sensitive indicators for climatic change. The purpose of this paper is to analyze and forecast the responses of snowmelt runoff to climate change. The upstream of Heihe River Basin in Northwestern China was chose as the representative catchments, and the observation data of the meteorological and hydrological stations were utilized to analyze the status and the regularity for the climatic change from 1956 to 2008. Moderate Resolution Imaging Spectroradiometer (MODIS) data were used to develop an optimized technology for snow mapping in the mountainous region. Snowmelt Runoff Model (SRM) was chose to simulate snowmelt runoff and scenario forecast the change trend of snowmelt runoff in catchment scale for the mountainous region in Northwestern China. The results show that climatic warming was apparent in the upstream of Heihe River Basin in the past 50a. Annual average air temperature of three different weather stations located in the basin has increased 2.1 °C, 2.6 °C and 2.9 °C, respectively. The snowmelt runoff has increased obviously from 1970 to present. With different warming climate scenarios, the results by SRM simulating showed that the first occurred time of snowmelt runoff shift ahead and discharge become larger as responses of snowmelt runoff to air temperature increasing, and the influence of temperature rising on average discharge of the whole snow season is not obvious. On the other hand, simulated discharge showed a marked increase trend with the increase of precipitation. And, the simulated results show that the increase of precipitation almost has no influence on the occurring time of snowmelt runoff.

1 Introduction

It was highlighted in IPCC reports (Solomon and Qin, 2007), that the global average surface temperature had a rise of 0.74 °C over the past 100 years. Global climate change had lead to the variation of snow cover distribution and snowmelt runoff in different scales, and also this variation will affect the management of snowmelt water resource. Many studies indicate that rising of temperature has caused redistribution and trended variations of snowcover at watershed scales in the Northern Hemisphere, High Asia, and mid-latitude mountains (McCabe and Wolock, 2009; López-Moreno et al., 2009). Water resources supply according to climate change is the most important issue in recent studies. These studies indicate that the discharge regime in snowmelt-dominated river basins is most sensitive to temperature increases in snow season (Rauscher et al., 2008; Adam et al., 2009; Day, 2009; Stewart et al., 2004). The earlier occurring of spring snowmelt runoff had been observed in many watersheds around the world (Bates, 2008; Lemke et al., 2007). With more than one-sixth of the Earth's population relying on glaciers and seasonal snow packs for their water supply, it is still needed to diagnose and predict the consequences of these hydrological changes for future water availability (Barnett et al., 2005).

Snow accumulation, distribution and ablation was surely be affected by climate change in Northwestern China. As the most important water resources in inland river basin such as Heihe River Basin in China, snowmelt runoff had received greater attention (Wang and Wang, 2003). As a result, the changes of snowmelt runoffs will directly affect redistribution of water resources, strategies and polices of water resources management, socio-economic development, industry and ecological environment (Wang and Li, 2006). Then, it is the most compelling need to study the response of snowmelt runoff to climatic change in Northwestern China.

The purpose of this article is to evaluate the responses of the snowcover and the snowmelt runoff to the climatic change, to simulate and forecast the change trend of snowmelt runoff for the mountainous region in Northwestern China.

2 Study area and data

The upstream of Heihe River Basin in Northwestern China, was chose as the study area (Fig. 1). Although Heihe River Basin is in the arid area, but the upper reaches of it has rich water resources derived from snow. The water supplies for the upper Heihe Watershed include snow- and ice-melt water, ground water and precipitation. The rainfall of the upper Heihe River Basin concentrates in summer, accounting for 61%–81% of annual total precipitation. However there is only 19% of annual total precipitation in spring season from March to June when the demands for agricultural irrigation are strongest. During this period, 70% of runoffs are supplied by snowmelt water (Wang and Li, 2001). Therefore, snowmelt and its variability will directly and remarkably affect the water supplies for agriculture, industry, and livestock in the middle and down streams of the Heihe River Basin. Climate change especially temperature increasing had affected greatly runoff in Heihe River Basin recently, and water resources distribution depends heavily on the snowmelt runoff. Overall, the upstream of Heihe River Basin is a typical inland river basin with seasonal snowpack, it is important to research the responses of air temperature, precipitation and runoff to climate change, and understand the inherent law of snowmelt runoff in the climate change scenario.

The basin area is about 10 009 km^2, with an altitude range from 1674 m to 5108 m. Temporary snow usually exists under 2700 m, patch snowpack is in range from 2700 m to 3400 m, continues and durative snowpack exists above 3400 m; Alpine steppe and desert steppe exists under 2800 m, alpine meadow and bushes is in range from 4000∼2800 m, bare ground exists above 4000 m (Wang and Li, 2006). There are 5 meteorological stations (MinLe, SuNan, QiLian, YeNiuGou, TuoLe) and 2 hydrological stations (ZhaMashike, YingLuoXia) distributed in the basin as Table 1 shows.

Snow Cover Area (SCA) is the key feature for expressing the distribution of snow in the temporal and special and also it is the vital inputs for the snowmelt runoff model. Remote sensing techniques can regularly and safely provide maps of snow cover area for the climate and hydrology model domain at a range of resolutions. In the last two decades, the snow maps have continually been improved as new satellite data have become available. The MODIS snow products (http://modis-snow-ice.gsfc.nasa.gov/atbd.html), available globally, are provided at a variety of different resolutions and projections to serve different user groups using a suite of automated algorithms (Hall et al., 2002; Riggs et al., 2006). The products are transferred to the National Snow and Ice Data Center (NSIDC) in Boulder, CO, where they are archived and distributed via the Warehouse Inventory Search Tool (WIST). In the study, the accuracy of MODIS snow products was analyzed in China. Using Terra MODIS Surface Reflectance data (MOD09) from 26 February 2000 to 16 October 2009, we described and validated a new method that retrieved daily snow-covered area in the upstream of Heihe River Basin.

3 Method

3.1 Snow cover mapping

Many results have suggested that MODIS snow cover products distributed by NSIDC agree well with surface observations, and the overall agreement is about 80–100% in flat topography (Klein and Barnett, 2003; Hall and Riggs, 2006). However, by comparison between MODIS daily snow product (MOD10A1) and snow depth data from climate stations located at mountainous regions in northern Xinjiang, it was found the MODIS snow products underestimated the snow cover area. A similar result is found by comparison between MOD10A1 and snow cover maps from Landsat-ETM+ (Hao et al., 2009). There are two main reasons for it, (1) Due to ignoring the effects of topography, the snow pixel shaded by mountain can not be identified from the MODIS snow products; (2) The distribution of snow depth is thin and patchiness in mountainous region, the characteristics affect the distinguishing in snow and free snow pixel. The snowpack in the upstream of Heihe River Basin belongs to mountainous snow cover. Thus, the algorithms of MODIS snow products need to be improved in this region.

HESSD

7, 493–528, 2010

3.1.1 Topographic correction of MODIS snow cover data

The research shows, in mountainous regions, without the terrain correction of a Digital Elevation Model (DEM), the snow cover area may be underestimated by the MODIS snow products. The new algorithm will correct the topographic effect by terrain correction models. There are many methods in terrain correction. Although physical models are quite successful to eliminate atmospheric and topographic effects, they inherently rely on an accurate spectral and radiometric sensor calibration and on the accuracy and appropriate spatial resolution of DEM in rugged terrain. In this method, an improved CIVCO model was used to eliminate terrain effect (Civco, 1989;Law and Nichol, 2004). The CIVCO method used here consists of two stages. In the first stage, shaded relief models, corresponding to the solar illumination conditions at the time of the satellite image are computed using the DEM data. This requires the input of the solar azimuth and altitude provided by the metadata of the satellite image. The resulting shaded relief model would have values between 0 and 1. Secondly, after the model is created, a transformation of each of the original bands of the satellite image is performed to derive topographically normalized images using Eqs. (1) and(2).

$$\delta \mathrm{Ref}_{\lambda ij} = \mathrm{Ref}_{\lambda ij} + \left[\mathrm{Ref}_{\lambda ij} \cdot \frac{(\mu_k - \mu_{ij})}{\mu_k} \cdot C_\lambda \right] \tag{1}$$

$$C_\lambda = \frac{S_\lambda - N_\lambda}{\left[\left(S_\lambda \cdot \frac{\mu_s - \mu_k}{\mu_k} \right) - \left(N_\lambda \cdot \frac{\mu_s - \mu_k}{\mu_k} \right) \right]} \tag{2}$$

Where,

$\delta\ \mathrm{Ref}_{\lambda ij}$=the normalized reflectance data for pixel (i,j) in band(λ)

$\mathrm{Ref}_{\lambda ij}$=the raw reflectance data for pixel (i,j) in band(λ)

μ_k=the mean illumination value for the entire scaled shaded relief model (0,1)

μ_{ij}=the scaled (0,1) illumination value for pixel(i,j)

C_λ=the correction coefficient for band (λ)

N_λ=the mean reflectance value on the slope facing away the sun

S_λ=the mean reflectance value on the slope facing to the sun

μ_k=the mean illumination value for the entire scaled shaded relief model (0.1)

μ_N=the mean scaled illumination value on the slope facing away the sun

μ_S=the mean scaled illumination value on the slope facing to the sun

By the topography correction, we can get the MODIS surface reflectance. It will improve the accuracy of snow cover mapping in the upstream of Heihe River Basin.

3.1.2 Change of the NDSI threshold value

The automated MODIS snow cover products algorithm is based on the evaluation of the normalized difference snow index (NDSI). In general, the NDSI is calculated as satellite reflectance in MODIS band 4 and 6:

$$\text{NDSI}=\frac{\text{band4}-\text{band6}}{\text{band4}+\text{band6}} \tag{3}$$

The NDSI threshold value of the MODIS snow cover products distributed by the NSIDC is 0.40. In general, the NDSI threshold value of the MODIS scenes greater than or equal to 0.40 represent snow cover pixels. In addition to the NDSI, many other threshold tests are used and described in many earlier publications (Hall et al., 1995, 2002).

However, validation of the current NDSI threshold has being accomplished just by the measurements in the US and Europe. In China, there is not reliable NDSI threshold value for mapping the MODIS snow cover area and a credible NDSI threshold value must be established. In the study, the three snow cover areas located at Xinjiang-TianShan mountainous and Qinghai-Tibet Plateau were selected for this study. First, the Landsat-ETM+ snow cover maps were produced by the method of the SNOMAP (Hall et al., 1995). Then, the snow cover maps, produced obtained from the way mentioned above, were compared with the ones derived by the manual photo interpretation classification technique. For the MODSI snow cover maps of the study areas, the NDSI threshold value for snow was increased gradually for 0.30 to 0.40 in steps of 0.01. At Last, the comparisons focused on comparing the MODIS snow cover maps following with NDSI threshold value and the Landsat-ETM+ snow cover maps serving as absolute standard. Table 3 shows the MODIS snow cover accuracy of different NDSI threshold in three regions. The result suggests that the MODIS snow cover products distributed by the NSIDC using NDSI threshold of 0.40 underestimated the SCA (snow-covered area) of the study areas. The credible NDSI threshold value is, respectively 0.34, 0.36 and 0.38 in the three regions. As computer the average value, it is approximately 0.36, which is less than the one from the 0.40 of NSIDC.

Figure 2 shows the flowchart of the new MODIS snow cover map algorithm. The daily MODIS SCA can be mapped by the new method. The new snow cover algorithm considered the effect of atmospheric and topographic conditions and improved the NDSI threshold value on the upstream of Heihe River Basin. The results showed it improved the identification accuracy and it is more accurate than algorithm of NSIDC on the upstream of Heihe River Basin.

3.2 SRM model

Snowmelt Runoff Model (SRM) was developed by Martinec (Martinec et al., 2005). It is designed to simulate and forecast daily runoff in mountainous basins where snowmelt is a major runoff component and it has also been applied to evaluate the effect of the changed climate on seasonal snow cover and runoff (Martinec et al., 2005). Nowadays, with advancing RS snow mapping technology the model has been applied in over 100 basins, and has more and more applications over the world. An obvious trend is using SRM to model response of runoff to climate change. The fundamental principle of SRM is to use degree-day factor algorithm as snow melt constraint, and to obtain the ratios of snow cover at watershed scale using remote sensing data, to assess discharge (Wang and Li, 2006).

The primary parameters of SRM include the snow cover area (SCA) from Satellite data, meteorological and hydrological measurement, and some other parameters such as the temperature lapse rate, degree-day factor and recession coefficient. There were detailed description and particular choice for these parameters in the past literature (Tekeli et al., 2005). In this paper, we mention how to confirm two key factors, the depletion curves of the snow cover area and the recession coefficient.

a. SCA Depletion Curves

Depletion curves of the snow cover area were interpolated from periodical snow cover mapping of MODIS which produced by the new SCA mapping algorithm with topographic correction and NDSI threshold value adjustment. The transitory new snow was accounted for as stored precipitation eventually contributing to runoff. The depletion curves of snow cover area are showed as Fig. 3. The basin was segmented as four elevation zones (A, B, C, and D). The zone A is almost no snow existence over the whole snow season.

b. Recession coefficient

Recession coefficient (k) indicates the decline of discharge in a period without snowmelt or rainfall, defined as (Martinec et al., 2008),

$$k_{n+1} = \frac{Q_{n+1}}{Q_n} \tag{4}$$

Where, Q_n is the discharge after n days. With the Recession flow logarithmical plot Q_n and Q_{n+1} of QiLian station and YinLuoXia station, the formulas of recession of two

HESSD

7, 493–528, 2010

Responses of snowmelt runoff to climatic change in an inland river basin

J. Wang et al.

stations were obtained, respectively,

QiLian station, $k_{n+1}=1.0324Q_n^{-0.0712}$

YinLuoXia station, $k_{n+1}=1.3619Q_n^{-0.1187}$

4 Snow cover area change in recent 10 years

The spatial and temporal variations of snow cover distribution on the upstream of Heihe River Basin could be acquired by obtained new MODIS daily snow cover maps. However, whether MODIS Terra or MODIS Aqua daily snow cover product, were all affected by clouds. The correlation of snow cover area variations with time could not be obtained using MODIS daily snow cover products due to the limitation of cloud cover. So the compositing technique will be used to obtain the SCA. A new 8-day composite maximum snow cover map is produced from daily MODIS snow cover map. A pixel is to be identified as the snow pixel in which if snow appears at least one day during the period of whole 8 days. The 8-day composite snow cover maps can minimize cloud cover and maximize the snow cover area. Figure 12a shows the snow cover area variations with different time in the upstream of Heihe River Basin from 24 February 2000 to 16 October 2009 by 8-day composite MODIS snow cover maps. By the same method, monthly and annual changes of SCA from 2000 to 2009 also were obtained. The result was showed in Fig. 12b and c. Results from various figures show that SCA has increased gradually in the recent 10 years on the upstream of Heihe River Basin. In 2008 the annual average SCA reached the peak of 2900 square kilometer. The result also shows the regional snowfall has an increase tendency year by year.

HESSD

7, 493–528, 2010

5 Analysis of the climate change in the past 50 years in the upstream of Heihe River Basin

5.1 Air temperature change

Air temperature has gradually increased with fluctuation over the past 50 years, which indicated by the change of the average annual air temperatures of the weather stations (Fig. 4). This increase trend is slow from 1956 to 1980 but enlarged after 1980a. At SuNan (2312 m) and MinLe (2271 m) stations located at lower altitudes, air temperature changes are similar with each other in the past. In this region, air temperature had an increase about 3 °C since 1980, and the average annual temperature had reached 4.5 °C in the recent 10 years; Climate conditions of middle zones of the basin could be represented by QiLian station (2787 m) which temperature change trend is similar with TuoLe Station (3360 m) at a higher altitude. The air temperature had changed a little in 1950s, but changed significantly after 1980s. Average air temperature of QiLian station had been greater than 1 °C in the past 12 years while it fluctuated around 1 °C before. Average air temperature had also increased to −2° in the past 10 years. The difference between maximum and minimum air temperature over the past 50 years, is about 2.1 °C at Qilian Station, 2.6 °C at YeNiuGou station and 2.9 °C at TuoLe Station.

5.2 Precipitation change

Annual precipitation of five meteorological stations varied from 250.8 mm to 395.6 mm as Fig. 5 shows. There are different increases ratio of precipitations at all five stations, in which the rising trends are more obvious at TuoLe and YeNiuGou station.

For understanding snowmelt responses to climate change, it is necessary to analysis the annual snowfall change trend in the snow seasons over the past years. Two meteorological stations, YeNiuGou and QiLian, were chose as the data sources. Spring and autumn snowfall were summed as the total snowfall each year. The increasing trends of snowfall of the 2 stations are close to each other in the past 50 years, in which the most obvious increase was from 1977 to 1986 with an increase of 100 mm. In recent 20 years, the increasing trend of snowfall is less obvious but with a large fluctuation about 70 mm.

5.3 Responses of snowmelt runoff to climate change

YingLuoXia station is the control section of the upstream of Heihe River basin. The discharge increased slowly from 1945 to 2008a, the minimum is 32.4 m^3/s of 1973 and the maximum is 73.3 m^3/s of 1989 (Fig. 6). The maximum monthly average discharge usually occurred at July or August, contributed mostly by rainfall (Fig. 7). By comparison of monthly discharge change in different years, it is found that the discharge in 1970s is lower than the other years, with a lower annual precipitation and lower average annual air temperature (Figs. 4 and 5). The total spring snowmelt discharge of 1980s is larger in all years. Snowmelt runoff of March and April increased obviously and peak discharge is earlier than ever before in recent 10 years, while the summer discharge is lower. Overall, the average annual discharge has an increasing trend and the inter-annual variation of peak discharges is large (Figs. 6 and 7). By comparison, discharge of QiLian station which located at middle altitude has an obviously increasing trend (Fig. 8). The maximum discharge occurred at 1989a, and the minimum occurred at 1979a. The comparison of monthly discharges showed that spring discharge has increased obviously from 1970 to present while the autumn discharge shift ahead and decreased (Fig. 9). Discharge from March to May was released mainly from snowpack in the upstream of Heihe River basin. With statistical data of YingLuoXia station and QiLian station from March to May (Figs.10 and 11), it was found that there are 3 period of the snowmelt runoff increases in this basin: 1950–1970, 1974–1989 and from 1999 to present. On the other hand, the peak spring discharge shifted ahead also, it agrees well with recorded observations (Wang and Li, 2001).

6 Scenario simulation and analysis of climate change by SRM

SRM model was used to simulate responses of snowmelt runoff to climate change, including several scenarios: increases of air temperature (+2 °C, +4 °C, +6 °C and heavier precipitation multiplied by 1.5 and 2 times. Firstly, the 2004 snowmelt season was simulated from 5 March to 19 July 2004. Two accuracy criterions, the coefficient recession flow determination and the volume difference are 0.02 and 7.1%, respectively. Then, the responses of snowmelt runoff to climate change were simulated based on this background. With increases of air temperature (+2 °C, +4 °C, +6 °C), the occurred time of peak snowmelt runoff shifted ahead and the discharge increased also (Fig. 13). The first peak discharge happened at 30 April 2004when there is no increase of air temperature. With an increase of +2 °C, the peak value increased from 102.8 m^3/s to 197.5 m^3/s and the start time of snowmelt runoff happened shifted not obviously; with an increase of +4 °C, the peak discharge increased to 167.1 m^3/s and the first time of it happened shifted ahead to 24 April; with an increase of +2 °C, the peak value of snowmelt runoff increased to 240.0 m^3/s and the first time of it happened shifted ahead to 21 April.

Earlier snowmelt runoff occurring and larger discharge are typical features of responses of snowmelt runoff to air temperature increasing, resulted from the analysis of a series of scenarios of air temperature changes. On the other hand, the aftereffect of advanced snowmelt is that the discharge of the later snow season becomes less and then discharge decreased correspondingly. With more increase of temperature, the discharge in later snow season decreased more. The other aftereffect of it is that the rain season comes ahead because precipitation happened as rain in higher temperature conditions, so the snowmelt confluence processes were affected also. In rain season, influence of temperature increase to runoff is small (Fig. 13). And, average daily runoff of the total snow season, are 47.8 m^3/s, 39.4 m^3/s, 35.0 m^3/s, 36.1 m^3/s, corresponds to 4 scenarios, respectively: present, +2 °C, +4 °C, +6 °C. As a result, the influence of temperature rising to average discharge of snow season is not obvious.

Assuming three scenarios of precipitation increases: be 1.5 times and 2 times of the origin precipitation, and precipitation multiplied by 2 times and with a +4 °C increase of air temperature (Fig. 14). Discharge process shown a marked increase trend with the increase of precipitation. The discharge was enlarged, but there are almost have no influence on the occurring time of snowmelt runoff, and the difference between precipitation fluctuation trends of different increased precipitation scenarios is not obvious. With comparison between 3 different scenarios, there is no obvious discharge change before the snow melting occurred in winter, while the discharge has been enlarged when the snowmelt season comes, and this amplification effect is more obvious in the mixed rain and snow season and the rainy season. The increased precipitation affected mainly on the expansion of the discharge. The average discharge increased from 47.8 m^3/s to 52.6 m^3/s and 67.9 m^3/s, with amplifications of 10% and 42%, respectively, when precipitation has increases of 1.5 times and 2 times.

Another climate change scenario is that precipitation multiplied by 2 times and with a +4 °C increase of air temperature (Fig. 14). This case could be considered as the comprehensive of air temperature and precipitation increases. The snowmelt runoff has a substantial advance and the peak discharge has greatly increased, but the discharge in later snow season is less than in the scenario of precipitation multiplied by 2 only. The average discharge is 67.0 m^3/s, it is closed to 67.9 m^3/s that the discharge of the scenario with single precipitation increase. It could be further concluded that the total runoff is mainly affected by precipitation other than air temperature.

7 Conclusions

Snow cover area is an important and sensitive input for snowmelt runoff hydrological model such as SRM. An improved snow cover mapping algorithm with NDSI index adjustment and topographic correction was designed to drive snow runoff modeling. The results showed that in the upstream of Heihe River Basin, air temperature has increased gradually in the recent 50 years, and the increase trend is slow from 1956 to 1980a but enlarged after 1980a. The increase of air temperature is about 2.1 °C, 2.6 °C and 2.9 °C at different weather stations located in the basin. Annual precipitation has increased also and the most marked rise period of precipitation was from 1977 to 1986. In recent 20 years, the increasing trend of snowfall is less obvious but with a large fluctuation. The comparison of monthly discharges showed that snowmelt runoff has increased obviously from 1970 to present while the autumn discharge hydrograph shifted ahead and the volume of it decreased.

Snowmelt runoff were simulated using SRM model in different climate change scenarios including: increases of air temperature (+2 °C, +4 °C, +6 °C) and heavier precipitation multiplied by 1.5 and 2 times. It was found that snowmelt runoff occurred earlier and discharges become larger as the responses of snowmelt runoff to air temperature increasing, and the influence of temperature rising to average discharge of snow season is not obvious. With increased precipitation, discharge hydrograph showed obvious increases of the volumes of peak discharges, but there almost is no influence on the occurring date of peak discharge. As a result, the total discharge is mainly affected by increase of precipitation other than air temperature.

Acknowledgements. This study was supported by National Natural Science Foundation of China (grant number: 40671040), CAS (Chinese Academy of Sciences) Action Plan for West Development Project "Watershed Allied Telemetry Experimental Research (WATER)" (grant number: KZCX2-XB2-09), and WP6 of FP7 topic ENV.2007.4.1.4.2 "Improving observing systems for water resource management".

References

Adam, J. C., Hamlet, A. F., and Lettenmaier, D. P.: Implications of global climate change for snowmelt hydrology in the twenty-first century, Hydrol. Process., 23, 962–972, 2009.
Barnett, T. P., Adam, J. C., and Lettenmaier, D. P.: Potential impacts of a warming climate on water availability in snow-dominated regions, Nature, 438, 303–309, 2005.
Bates, B. C., Kundzewicz, Z. W., Wu, S., and Palutik, J. P.: Climate Change and Water, IPCC

Secretariat, Geneva, Technical Paper of the Intergovernmental Panel on Climate Change, 210 pp., 2008.

Civco, D. L.: Topographic normalization of landsat Thematic Mapper digital imagery, Photogramm Eng. Rem. S., 55, 1303–1309, 1989.

Day, C. A.: Modelling impacts of climate change on snowmelt runoff generation and streamflow across western US mountain basins: a review of techniques and applications for water resource management, Prog. Phys. Geog., 33, 614–633, 2009.

Hall, D. K., Riggs, G. A., Salomonson, V. V.: Development of methods for mapping global snow cover using Moderate Resolution Imaging Spectroradiometer (MODIS) data, Remote Sens. Environ., 54, 127–140, 1995.

Hall, D. K., Riggs, G. A., Salomonson, V. V., et al.: MODIS snow-cover products, Remote Sens. Environ., 83, 181–194, 2002.

Hall, D. K. and Riggs, G. A.: Accuracy assessment of the MODIS snow products, 63rd Eastern Snow Conference, Newark, DE, 1534–1547, 2007.

Hao, X., Zhang, P., and Wang, J.: Evaluation and comparison of MODIS and VEGETATION Snow Cover products in Northern Xinjiang, China, Remote sensing technology and application, 24, 603–610, 2009(in Chinese).

Klein, A. G. and Barnett, A. C.: Validation of daily MODIS snow cover maps of the Upper Rio Grande River Basin for the 2000–2001 snow year, Remote Sens. Environ., 86, 162–176, 2003.

López-Moreno, J. I., Goyette, S., and Beniston, M.: Impact of climate change on snowpack in the Pyrenees: Horizontal spatial variability and vertical gradients, J. Hydrol., 374, 384–396, 2009.

Law, K. H. and Nichol, J.: Topographic correction for differential illumination effects on IKONS satellite imagery, ISPRS Congress, 12–23 July 2004 Istanbul, Turkey Commission 3.

Lemke, P., Ren., J., Alley., R. B., Allison., I., Carrasco., J., Flato., G., Fujii., Y., Kaser., G., Mote., P., Thomas., R. H., and Zhang., T.: Observations: Changes in Snow, Ice and Frozen Ground, Contribution of Working Group I to the Fourth Assessment Report of the Intergovernmental Panel on Climate Change, Cambridge, United Kingdom and New York, NY, USA, 2007.

Martinec, J., Rango, A., and Roberts, R.: SRM (Snowmelt Runoff Model)User's Manual, Las Cruces, New Mexico: New Mexico State University, 175 pp., 2008.

McCabe, G. J. and Wolock, D. M.: Recent Declines in Western U.S. Snowpack in the Context of Twentieth-Century Climate Variability, Earth Interact., 13, 1–15, 2009.

Rauscher, S. A., Pal, J. S., Diffenbaugh, N. S., and Benedetti, M. M.: Future changes in snowmelt-driven runoff timing over the western US, Geophys. Res. Lett., 35, L16703, doi:10.1029/2008gl034424, 2008.

Riggs, G. A., Hall, D. K, and Salomonson, V. V.: MODIS Snow Products User Guide Collection 5., http://modis-snow-ice.gsfc.nasa.gov/sugkc2.html, 2006.

Solomon, S., Qin, D., M. Marquis, Z. C., Averyt, K. B., Tignor, M., and Miller, H. L.(Eds.): Climate change 2007: the physical science basis: contribution of Working Group I to the Fourth Assessment Report of the Intergovernmental Panel on Climate Change, Cambridge University Press, Cambridge, New York, 2007.

Stewart, I. T., Cayan, D. R., and Dettinger, M. D.: Changes in snowmelt runoff timing in western North America under a "business as usual" climate change scenario, Clim. Change, 62, 217–232, 2004.

Tekeli, A. E., Akyurek, Z., Sorman, A. A., Sensoy, A., and Sorman, A. U.: Using MODIS snow cover maps in modeling snowmelt runoff process in the eastern part of Turkey, Remote Sens. Environ., 97, 216–230, 2005.

Wang, J. and Li, W.: Establishing snowmelt runoff simulating model using remote sensing data and GIS in the west of China, Int. J. Remote Sens., 22, 3267–3274, 2001.

Wang, J. and Wang, L. H.: A review on snow cover and snowmelt runoff simulating using remote sensing data sets in China, P. Soc. Photo-Opt. Ins., 4894, 446–455, 2003.

Wang, J. and Li, S.: Effect of climatic change on snowmelt runoffs in mountainous regions of inland rivers in Northwestern China, Sci. China Ser. D., 49, 881–888, 2006.

HESSD
7, 493–528, 2010

Responses of snowmelt runoff to climatic change in an inland river basin

J. Wang et al.

Table 1. Basic information of meteorological stations in the upstream of Heihe River Basin.

Station	Longitude	Latitude	Elevation/m	Air temperature/°	Annual precipitation/mm
MinLe	100°49′	38°27′	2271	3.4	335.4
SuNan	99°37′	38°48′	2312	3.9	250.8
QiLian	100°14′	38°12′	2787	1.1	395.6
YeNiuGou	990°36′	38°24′	3180	−2.9	376.6
TuoLe	98°24′	38°48′	3360	−2.5	259.4

Table 2. Elevation zones of the upstream of Heihe River Basin.

Elevation zone	Elevation range/m	Area/km^2	Average Elevation/m
A	1700~2700	423.49	2456
B	2700~3400	2195.44	3156
C	3400~4000	4641.18	3719
D	4000~5108	2748.89	4196
Whole Basin	1700~5108	10009.00	–

HESSD
7, 493–528, 2010

Responses of snowmelt runoff to climatic change in an inland river basin

J. Wang et al.

Table 3. MODIS snow cover accuracy of different NDSI threshold in three regions in Northwestern China.

NDSI threshold value	The overall accuracy, Kappa coefficient and fractional snow cover area of A region.	The overall accuracy, Kappa coefficient and fractional snow cover area of B region.	The overall accuracy, Kappa coefficient and fractional snow cover area of C region.
0.39	93.00%, 0.669, 11.37%	86.82%, 0.676, 27.73%	94.73%, 0.708, 10.17%
0.38	93.02%, 0.672, 11.53%	86.81%, 0.678, 28.36%	94.74%, 0.711, 10.48%
0.37	93.07%, 0.675, 11.66%	86.76%, 0.679, 29.02%	94.62%, 0.709, 10.79%
0.36	93.11%, 0.679, 11.83%	86.73%, 0.680, 29.63%	94.51%, 0.707, 11.08%
0.35	93.16%, 0.683, 11.97%	86.63%, 0.679, 30.25%	94.39%, 0.706, 11.48%
0.34	93.17%, 0.685, 12.13%	86.54%, 0.679, 30.87%	94.26%, 0.703, 11.82%
0.33	92.89%, 0.678, 12.66%	86.45%, 0.679, 31.51%	94.16%, 0.702, 12.16%
0.32	92.91%, 0.681, 12.80%	86.28%, 0.677, 32.13%	94.04%, 0.700, 12.53%
0.31	92.91%, 0.683, 12.98%	86.13%, 0.676, 32.66%	93.88%, 0.697, 12.89%
0.30	92.90%, 0.684, 13.18%	86.05%, 0.676, 33.23%	93.69%, 0.692, 13.28%

(a) The SCA variations of every 8-day of the upstream of Heihe River Basin

(b) The monthly average variations of SCA of the upstream of Heihe River Basin

(c) The annual average variations of SCA of the upstream of Heihe River Basin

HESSD

7, 493–528, 2010

Title Page
Abstract | Introduction
Conclusions | References
Tables | Figures
◀◀ | ▶▶
◀ | ▶
Back | Close
Full Screen / Esc
Printer-friendly Version
Interactive Discussion

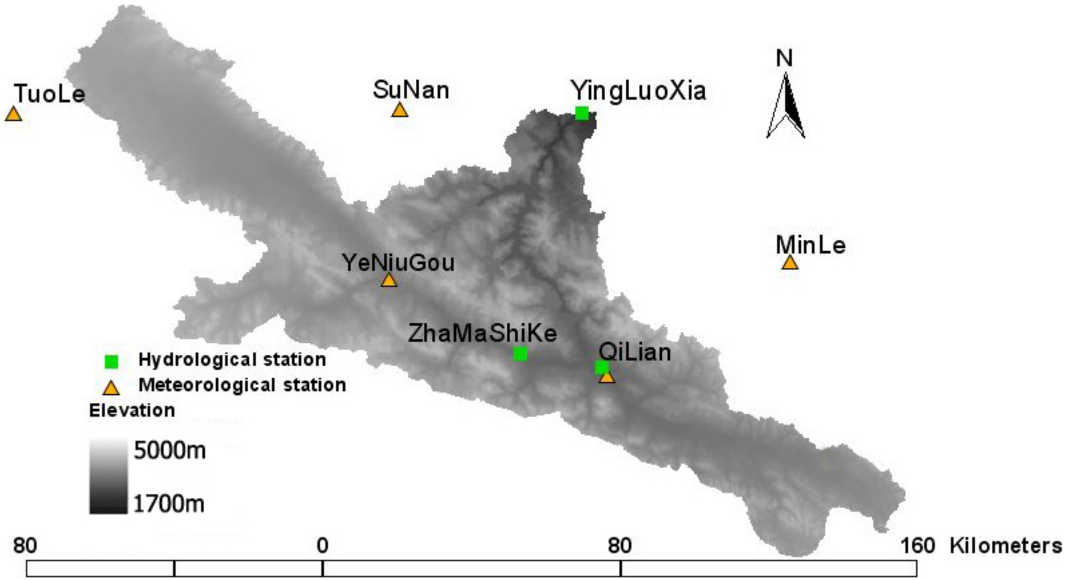

Fig. 1. Map of the upstream of Heihe River Basin.

HESSD
7, 493–528, 2010

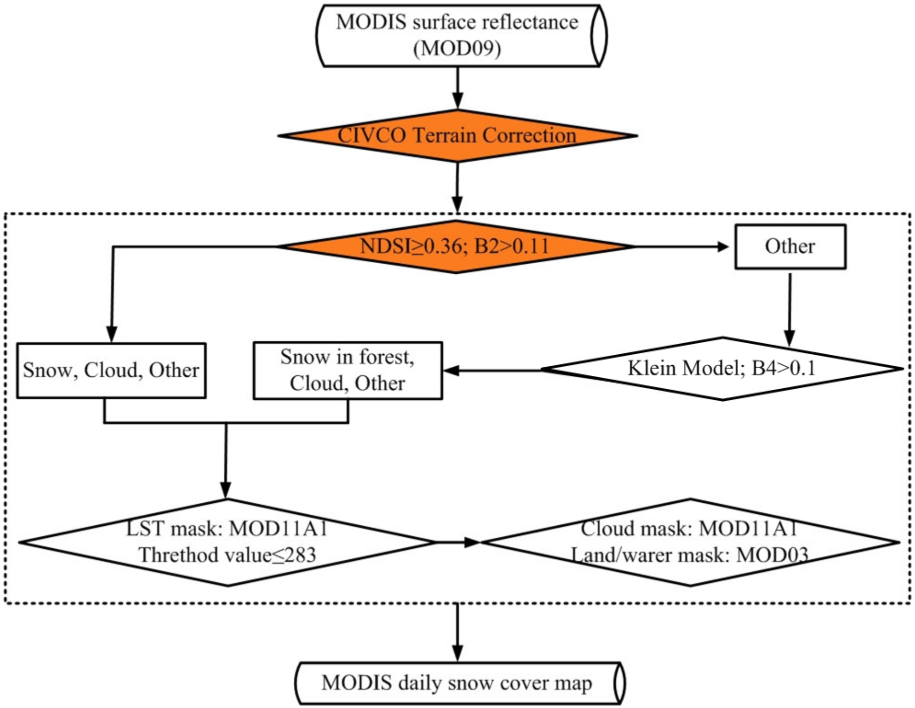

Fig. 2. The flow process of new MODIS daily snow cover map algorithm.

HESSD
7, 493–528, 2010

Responses of snowmelt runoff to climatic change in an inland river basin

J. Wang et al.

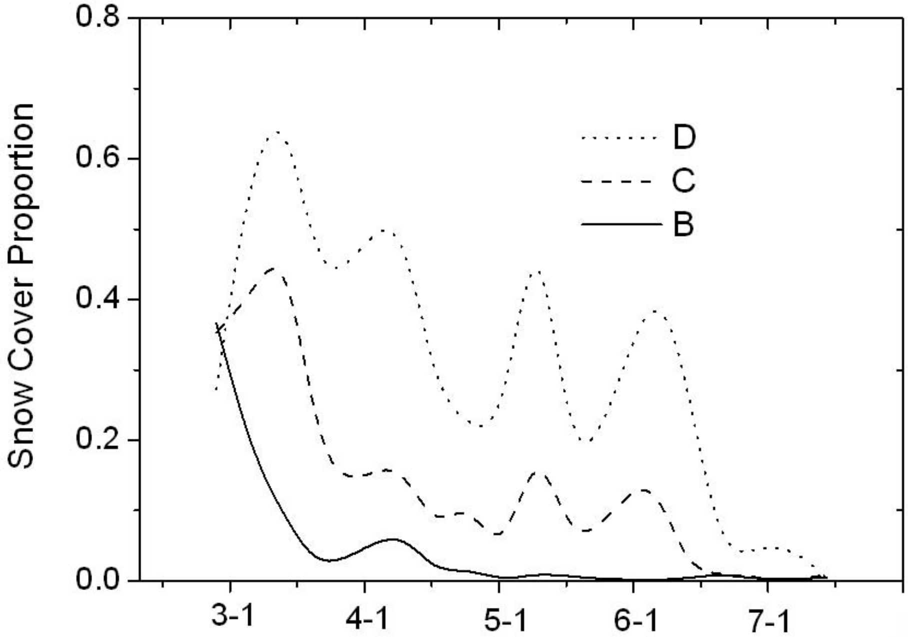

Fig. 3. Depletion curves of the snow coverage for the elevation zones of the upper Heihe Basin from MODIS data during the snowmelt season in 2004.

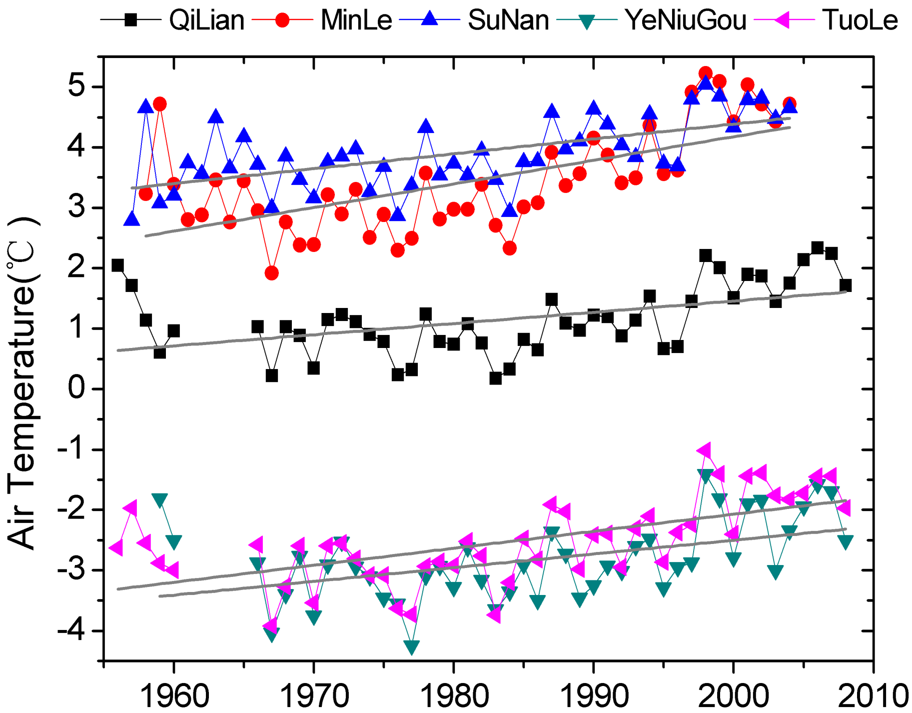

Fig. 4. Change of the average annual air temperatures of weather stations in the past 50 years.

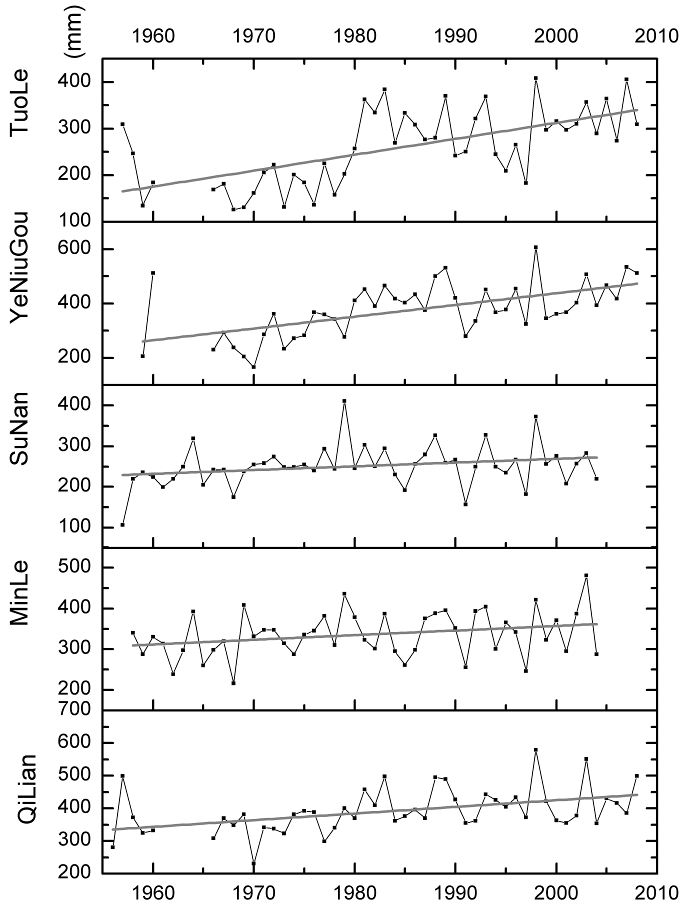

Fig. 5. Annual precipitation of 5 meteorological stations (1956–2008).

HESSD
7, 493–528, 2010

Responses of snowmelt runoff to climatic change in an inland river basin

J. Wang et al.

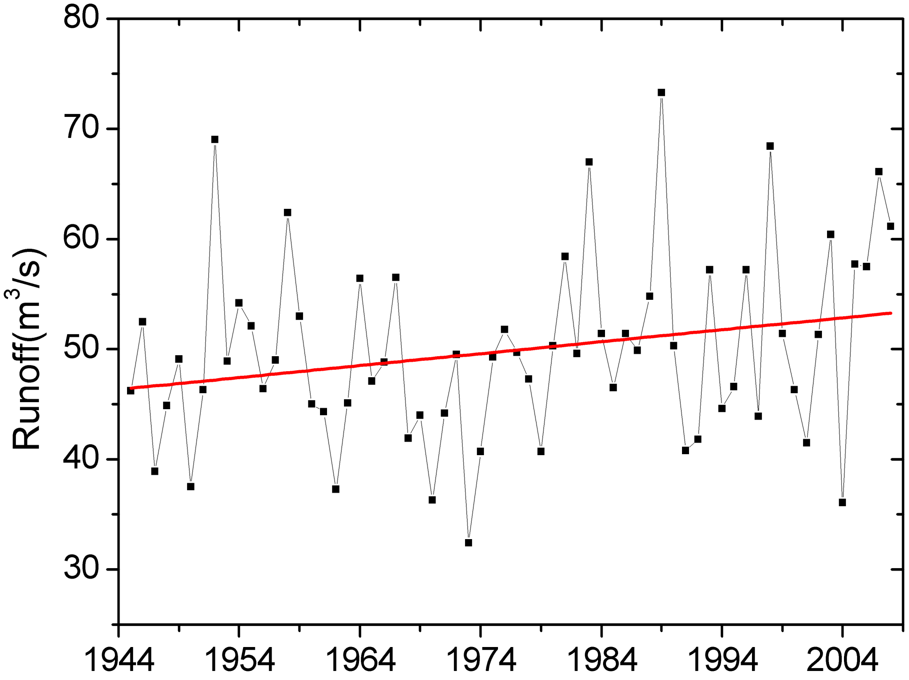

Fig. 6. Average annual runoff of YingLuoXia hydrologic station.

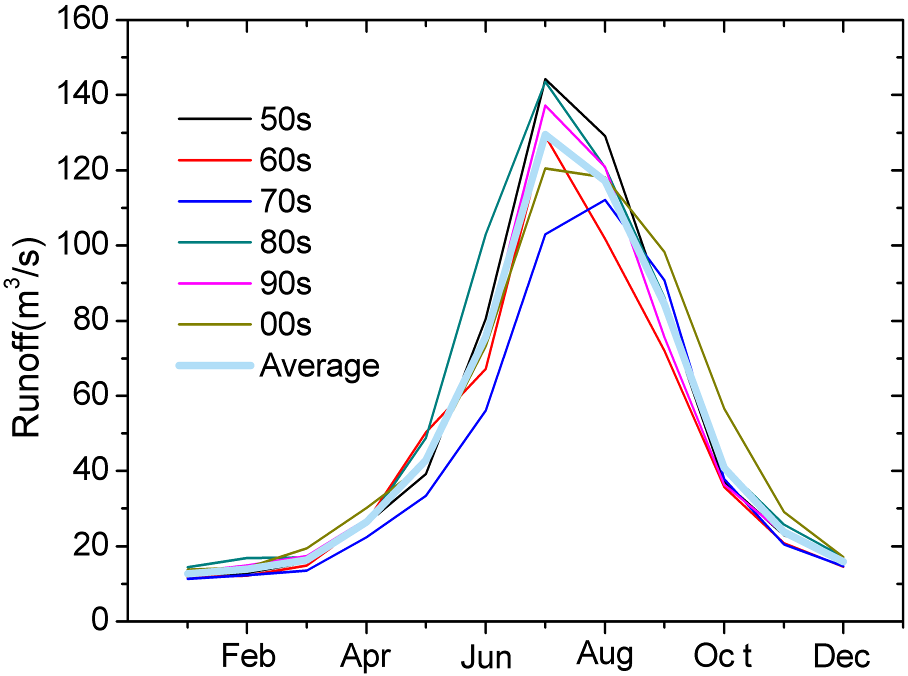

Fig. 7. Average monthly runoff change of YingLuoXia station from 1950s to present.

HESSD
7, 493–528, 2010

Responses of snowmelt runoff to climatic change in an inland river basin

J. Wang et al.

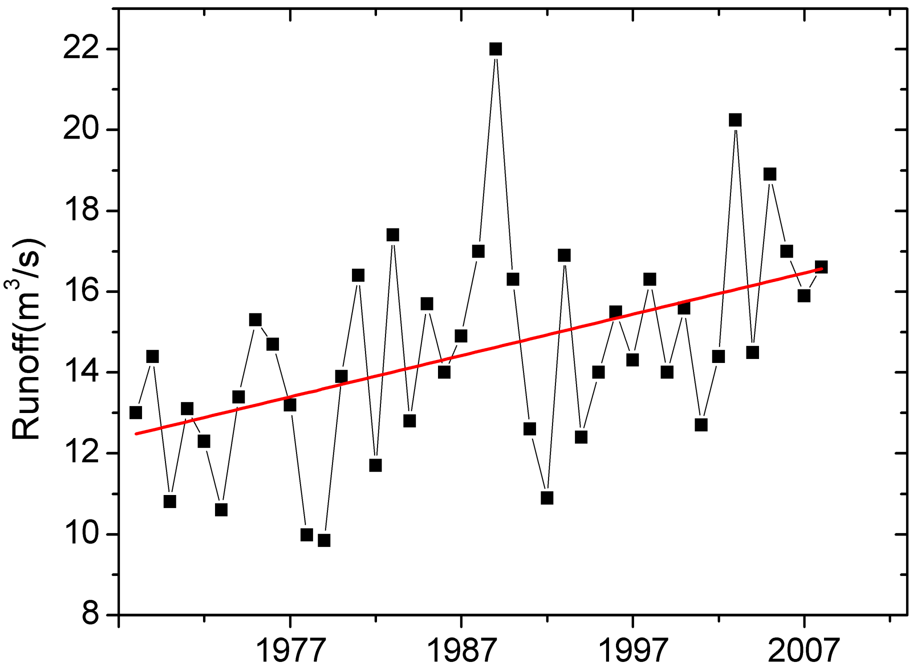

Fig. 8. Average annual runoff of QiLian station.

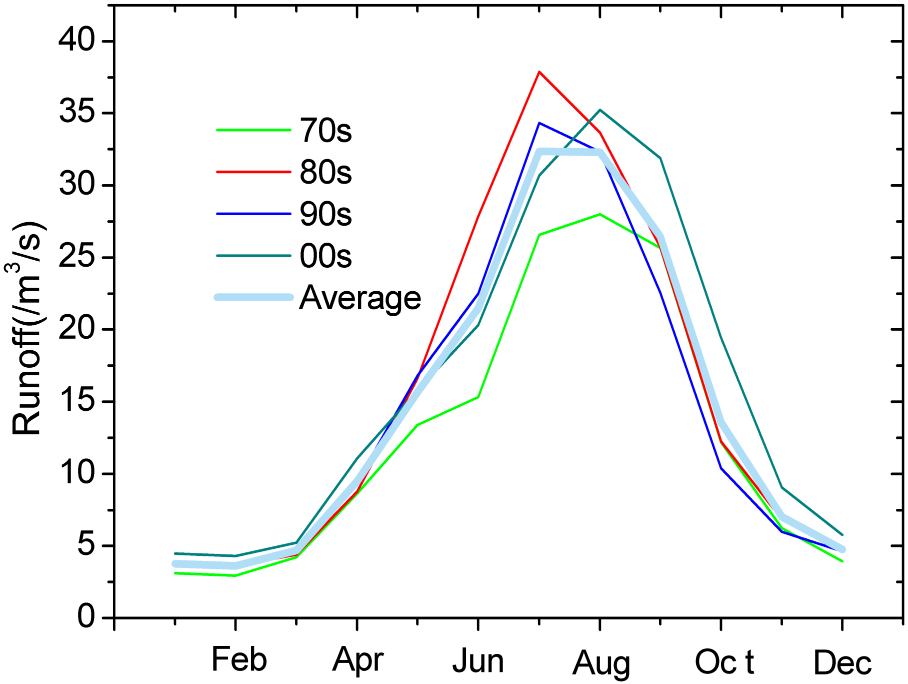

Fig. 9. Average monthly runoff change of QiLian station.

HESSD

7, 493–528, 2010

Responses of snowmelt runoff to climatic change in an inland river basin

J. Wang et al.

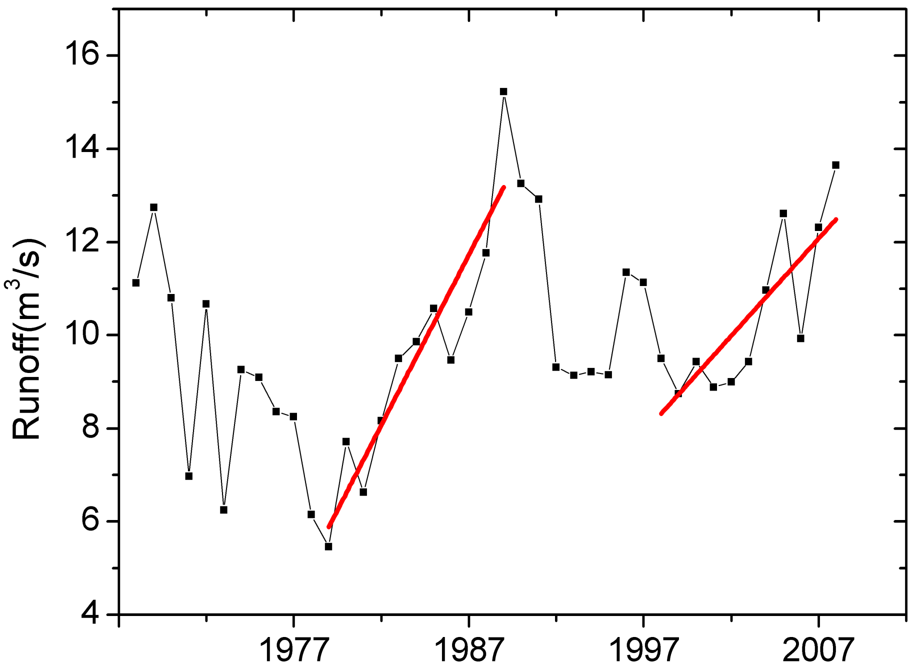

Fig. 10. Monthly spring snowmelt runoff change of QiLian station (March to May).

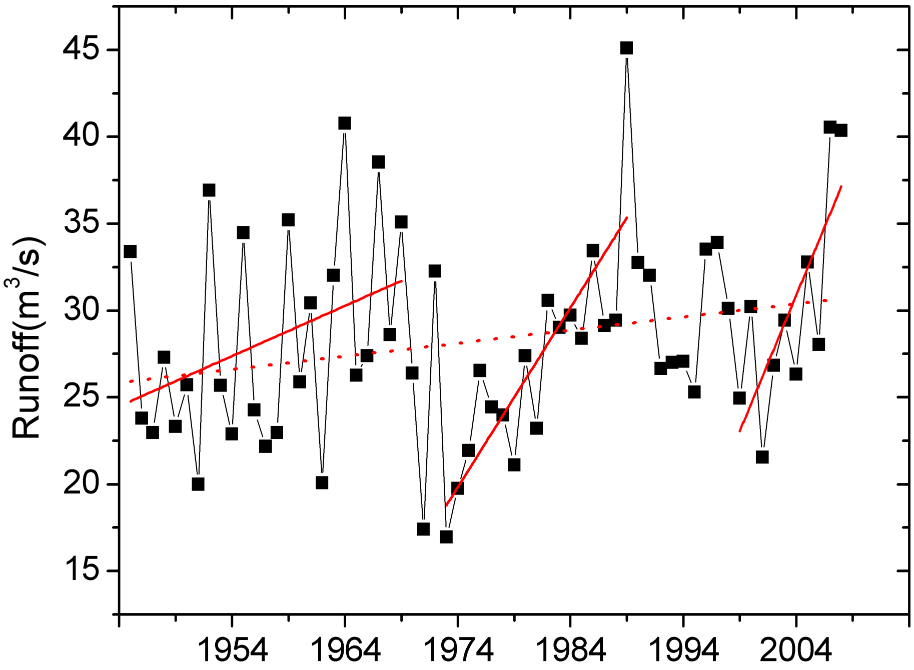

Fig. 11. Monthly spring snowmelt runoff change of YingLuoXia station (March to May).

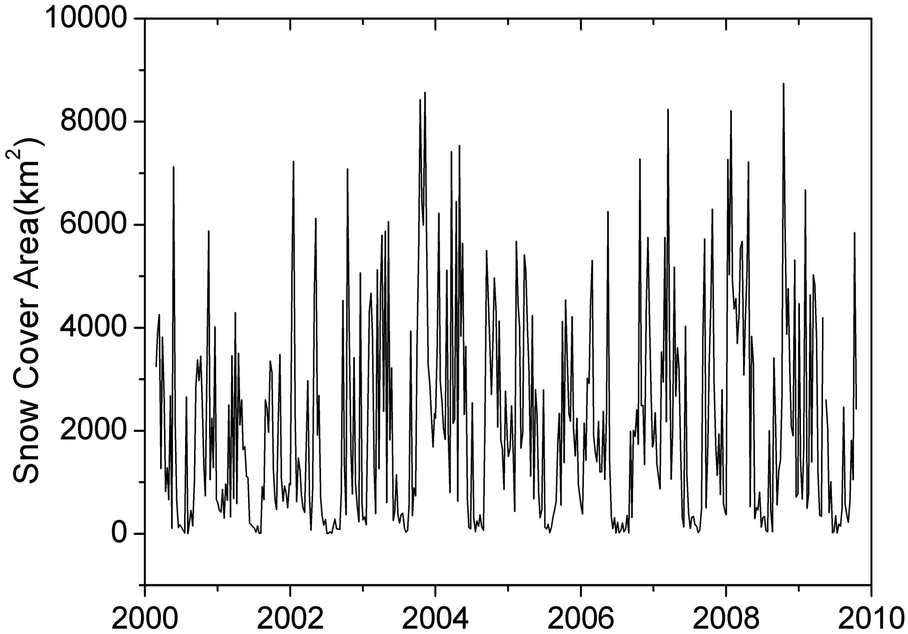

Fig. 12a. The SCA variations of every 8-day of the upstream of Heihe River Basin.

HESSD
7, 493–528, 2010

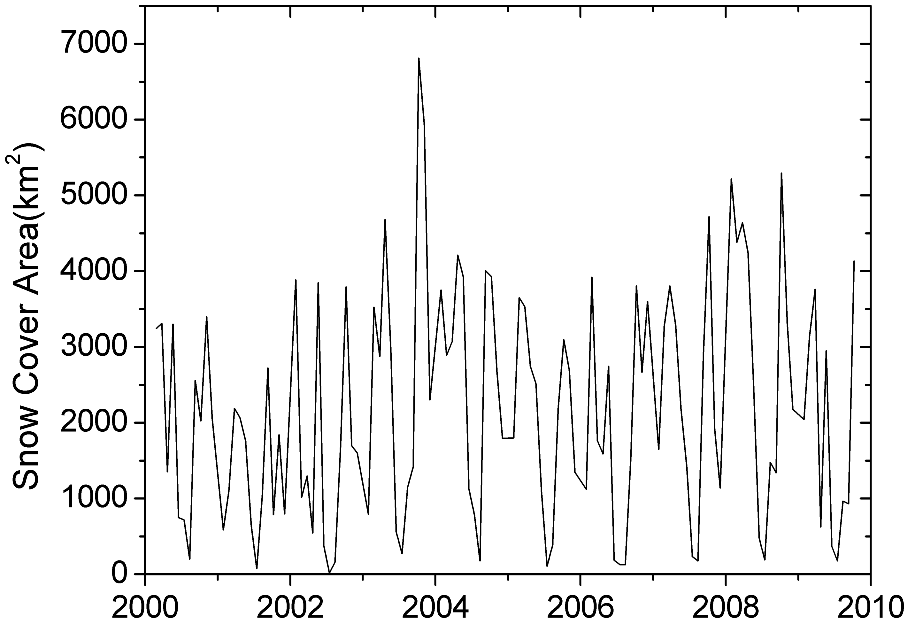

Fig. 12b. The monthly average variations of SCA of the upstream of Heihe River Basin.

HESSD
7, 493–528, 2010

Responses of snowmelt runoff to climatic change in an inland river basin

J. Wang et al.

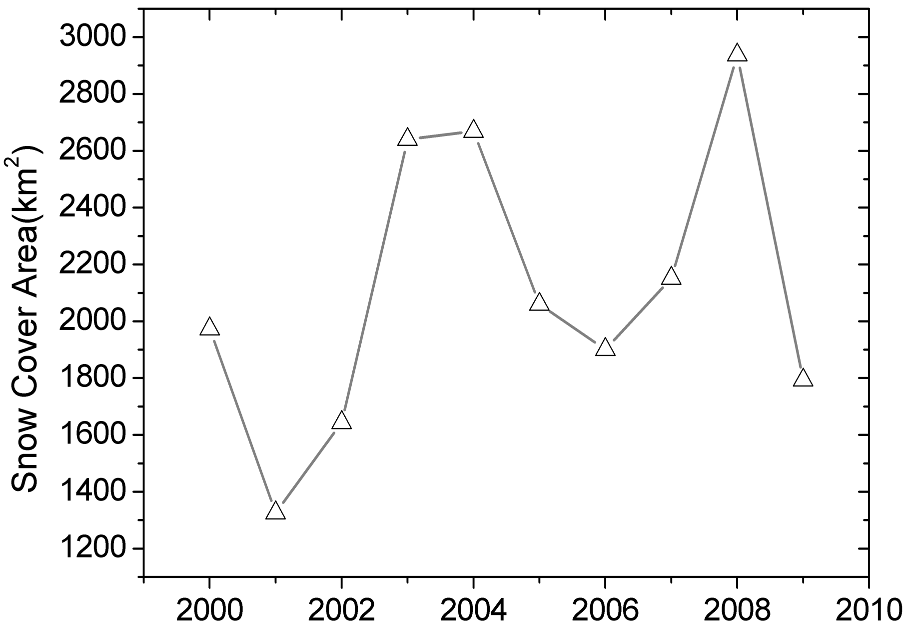

Fig. 12c. The SCA variations with time of the upstream of Heihe River Basin from 24 February 2000 to 16 October 2009 by 8-day composed MODIS snow cover data.

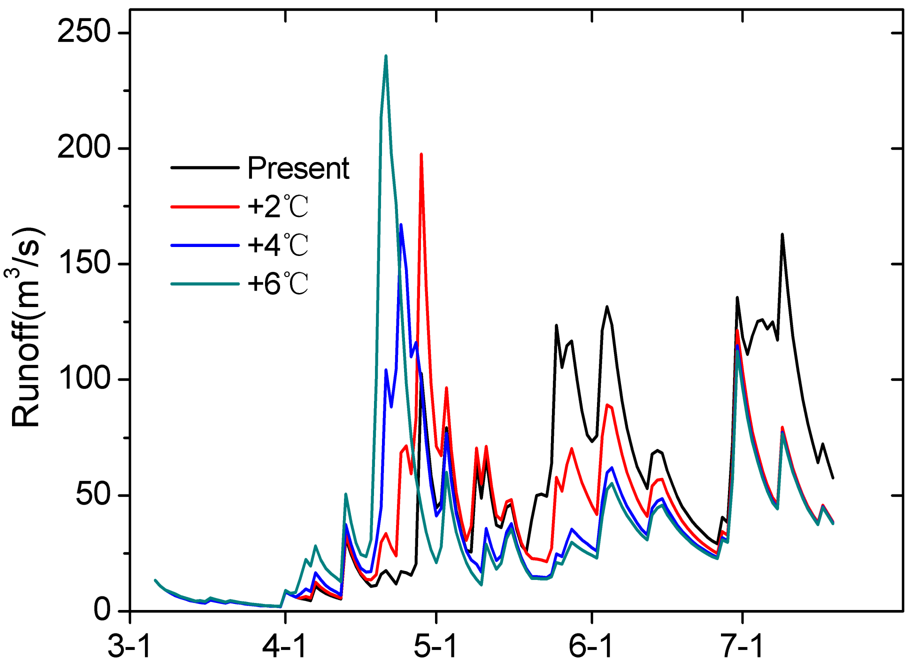

Fig. 13. Responses of snowmelt runoff to air temperature increases, +2 °C, +4 °C, +6 °C.

HESSD

7, 493–528, 2010

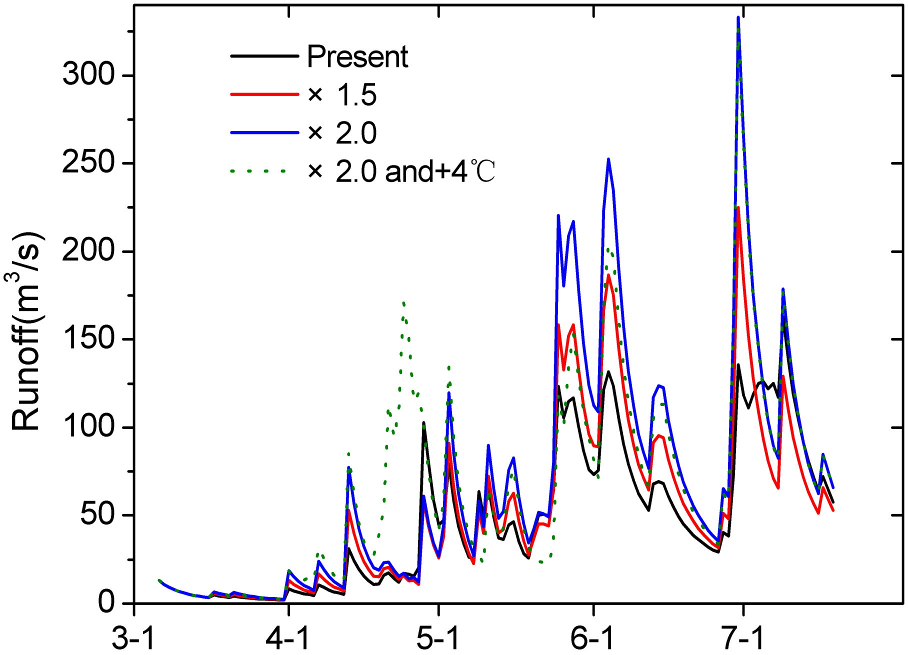

Fig. 14. Responses of snowmelt runoff to three different scenarios: precipitation multiplied by 1.5 and 2 times, and precipitation multiplied by 2 times and with a +4 °C increase of air temperature.